Serial proton MR spectroscopy of gray and white matter in relapsing-remitting MS

Ivan I. Kirov, PhD
Assaf Tal, PhD
James S. Babb, PhD
Joseph Herbert, MD
Oded Gonen, PhD

Correspondence to
Dr. Gonen:
oded.gonen@med.nyu.edu

ABSTRACT

Objective: To characterize and follow the diffuse gray and white matter (GM/WM) metabolic abnormalities in early relapsing-remitting multiple sclerosis using proton magnetic resonance spectroscopic imaging (^{1}H-MRSI).

Methods: Eighteen recently diagnosed, mildly disabled patients (mean baseline time from diagnosis 32 months, mean Expanded Disability Status Scale [EDSS] score 1.3), all on immunomodulatory medication, were scanned semiannually for 3 years with T1-weighted and T2-weighted MRI and 3D ^{1}H-MRSI at 3 T. Ten sex- and age-matched controls were followed annually. Global absolute concentrations of *N*-acetylaspartate (NAA), choline (Cho), creatine (Cr), and *myo*-inositol (mI) were obtained for all GM and WM in the 360 cm^3 ^{1}H-MRSI volume of interest.

Results: Patients' average WM Cr, Cho, and mI concentrations (over all time points), 5.3 ± 0.4, 1.6 ± 0.1, and 5.1 ± 0.7 mM, were 8%, 12%, and 11% higher than controls' ($p \leq 0.01$), while their WM NAA, 7.4 ± 0.7 mM, was 6% lower ($p = 0.07$). There were increases with time of patients' WM Cr: 0.1 mM/year, Cho: 0.02 mM/year, and NAA: 0.1 mM/year (all $p < 0.05$). None of the patients' metabolic concentrations correlated with their EDSS score, relapse rate, GM/WM/CSF fractions, or lesion volume.

Conclusions: Diffuse WM glial abnormalities were larger in magnitude than the axonal abnormalities and increased over time independently of conventional clinical or imaging metrics and despite immunomodulatory treatment. In contrast, the axonal abnormalities showed partial recovery, suggesting that patients' lower WM NAA levels represented a dysfunction, which may abate with treatment. Absence of detectable diffuse changes in GM suggests that injury there is minimal, focal, or heterogeneous between cortex and deep GM nuclei. *Neurology*® 2013;80:1–8

GLOSSARY

Cho = choline; **Cr** = creatine; **EDSS** = Expanded Disability Status Scale; **FLAIR** = fluid-attenuated inversion recovery; **GM** = gray matter; **^{1}H-MRS** = proton magnetic resonance spectroscopy; **^{1}H-MRSI** = proton magnetic resonance spectroscopic imaging; **mI** = *myo*-inositol; **MPRAGE** = magnetization-prepared rapid gradient echo; **MS** = multiple sclerosis; **NAA** = *N*-acetylaspartate; **RRMS** = relapsing-remitting multiple sclerosis; **VOI** = volume of interest; **WM** = white matter.

In multiple sclerosis (MS), conventional MRI is sensitive to gray and white matter (GM/WM) atrophy and can distinguish active from chronic lesions, but lacks specificity to gliosis, inflammation, demyelination, and neuronal loss.[1] These can be examined with proton magnetic resonance spectroscopy (^{1}H-MRS) quantification of *N*-acetylaspartate (NAA) for neuronal health, creatine (Cr) for glial cell density, choline (Cho) for membrane turnover, and *myo*-inositol (mI) for astrocyte status.[2] However, the utility of ^{1}H-MRS in understanding MS evolution is limited by technological and cost constraints to mostly cross-sectional investigations.[1] Although conclusions on disease course are drawn from such studies, only follow-up allows direct observation of disease progress. Therefore, there is a reiterated need for longitudinal ^{1}H-MRS, in particular of diffuse pathology in normal-appearing tissue.[3,4]

We report findings from a 3-year semiannual ^{1}H-MRS follow-up of recently diagnosed patients with relapsing-remitting MS (RRMS). We also address the common ^{1}H-MRS pitfalls: low sensitivity, partial volume,[5] and quantification with metabolite ratios.[3] Specifically, for maximum sensitivity

Editorial, page XXX

Supplemental data at www.neurology.org

From the Departments of Radiology (I.I.K., A.T., J.S.B., O.G.) and Neurology (J.H.), New York University School of Medicine, New York, NY.
Go to Neurology.org for full disclosures. Funding information and disclosures deemed relevant by the authors, if any, are provided at the end of the article.

to diffuse changes, we estimated the global metabolic concentrations in the GM and WM of a ~0.4 L volume of interest (VOI), larger than in any previous serial study. Partial volume effects were removed by using multivoxel, high spatial resolution (0.75 cm^3) 3D proton magnetic resonance spectroscopic imaging (^{1}H-MRSI), correcting each voxel for tissue fractions from coregistered segmented MRI. Our previous cross-sectional, non-tissue-specific study showing diffuse glial abnormalities, without neuronal dysfunction,[6] motivated us to define metabolism by tissue type and establish its temporal course in the same cohort.

METHODS Human subjects. Twenty-nine patients (9 men, 20 women) with clinically definite RRMS[7] for less than 6 years were recruited prospectively to be scanned semiannually for 3 years (7 scans each). Exclusion criteria at enrollment were the

Figure 1 Positioning of the ^{1}H-MRSI volume of interest and example spectra

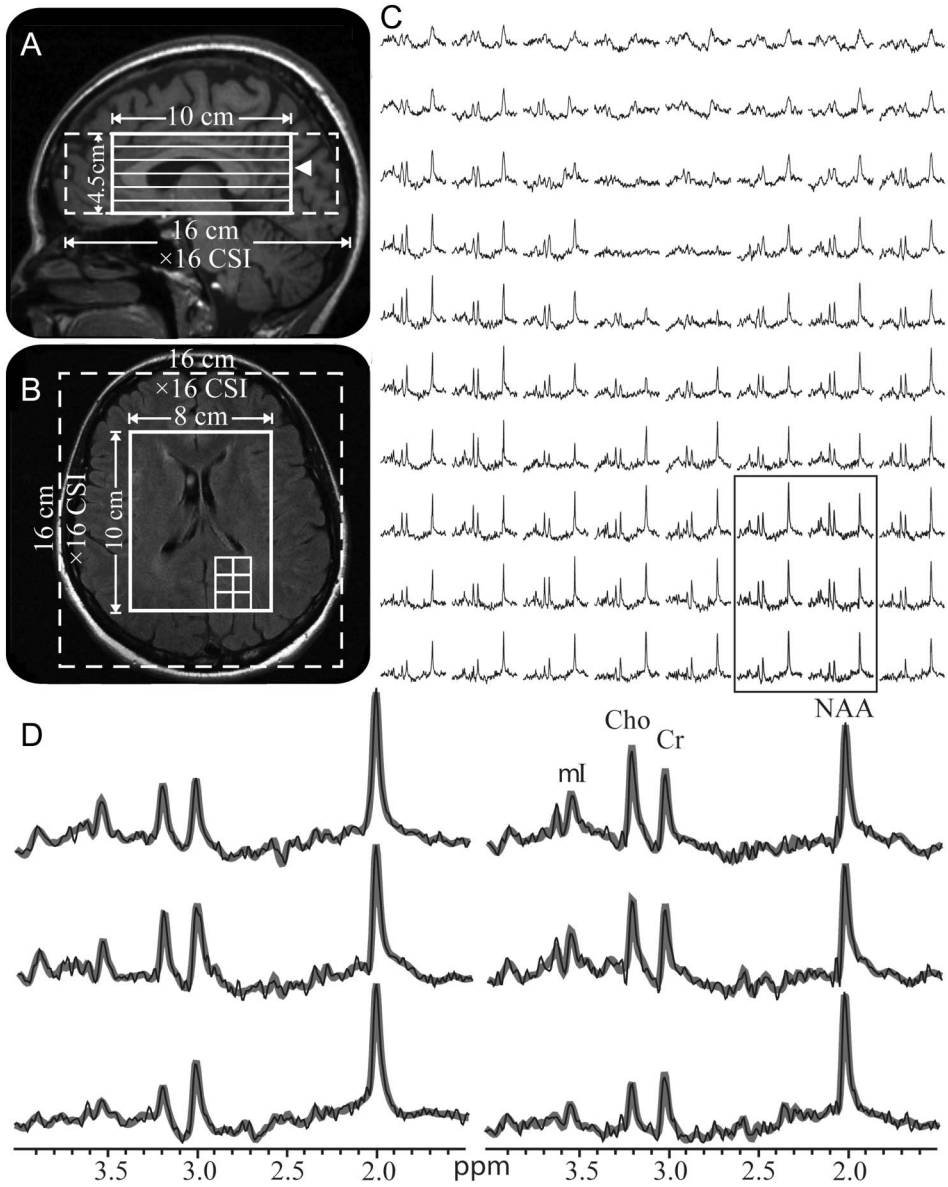

Sagittal T1-weighted magnetization-prepared rapid gradient echo (A) and axial T2-weighted fluid-attenuated inversion recovery (B) of patient 8 in the table, superimposed with the volume of interest (VOI) and field of view (solid and dashed white frames). The location of (B) is indicated on (A) by an arrowhead. (C) Real part of the 8 × 10 (LR × AP) ^{1}H spectra matrix from the VOI on (B), on common 1.4–3.8 ppm and intensity scales. Note the consistent spectral quality in these 0.75 cm^3 voxels acquired in ~30 minutes of acquisition. (D) Expanded and magnified spectra from the 6 spectroscopic voxels, delineated in (B) and (C), superimposed with their fitted model functions (gray lines). Note the spectral resolution and the fidelity of the fitting procedure. Cho = choline; Cr = creatine; ^{1}H-MRSI = proton magnetic resonance spectroscopic imaging; mI = *myo*-inositol; NAA = *N*-acetylaspartate.

Table Patient demographic data at baseline and EDSS and medications at 0 (baseline), 12, 24, and 36 months

Patient	Age, y/sex	Months from diagnosis	EDSS				Medication			
			0	12	24	36	0	12	24	36
1	38/M	2	2.0	2.0	2.5	2.5	GA			
2	27/F	12	1.0	0.0	1.5	1.5	IFN-β-1b	N-mab		
3	38/M	15	0.0	1.0	2.0	2.0	IFN-β-1a	IFN-β-1a	—	
4	30/M	17	0.0	0.0	0.0	0.0	GA			
5	35/F	18	1.0	1.5	—	1.5	IFN-β-1a			
6	38/F	18	0.0	—	0.0	1.0	IFN-β-1a			
7	34/F	18	0.0	—	0.0	0.0	IFN-β-1a			
8	37/F	23	0.0	2.0	0.0	0.0	GA			
9	33/M	24	1.0	1.0	1.0	0.0	IFN-β-1a			
10	30/F	25	5.5	—	5.0	3.0	IFN-β-1b			
11	21/F	28	1.5	—	1.5	1.5	—		IFN-β-1a	IFN-β-1b
12	32/F	32	1.0	2.0	2.0	3.0	IFN-β-1b, IVIg			
13	29/F	38	1.0	—	0.0	1.0	GA			
14	26/F	49	3.0	—	2.0	1.0	GA	N-mab		IVIg
15	41/F	56	1.0	1.5	1.0	3.0	IFN-β-1a			
16	38/F	59	2.0	2.0	1.5	—	IFN-β-1a			
17	31/F	62	2.0	1.5	1.0	0.0	IFN-β-1a			
18	38/M	75	1.0	1.0	0.0	3.5	IFN-β-1a		IFN-β-1a, IVIg	
Average	33	32	1.3	1.3	1.3	1.4				

Abbreviations: EDSS = Expended Disability Status Scale; GA = glatiramer acetate; IFN = interferon; IVIg = IV immunoglobulin; N-mab = natalizumab.

usual MRI contraindications, alcohol or drug abuse, inability to provide consent, HIV infection, or history of psychiatric or other neurologic disease. Ten age- and sex-matched (2 men, 8 women) healthy volunteers with identical exclusion criteria, but also including unremarkable MRI, were to be scanned annually (4 scans each). Post hoc exclusion criterion was less than 5 scans for patients and less than 4 for controls.

Standard protocol approvals, registrations, and patient consents. This study was approved by the Institutional Review Board of New York University School of Medicine and written informed consent was obtained from all participants.

Data acquisition. All measurements were done in a 3T magnetic resonance scanner (appendix e-1 on the *Neurology*® Web site at www.neurology.org). Sagittal 3D magnetization-prepared rapid gradient echo (MPRAGE) images were acquired for MRSI VOI guidance and for tissue segmentation and axial T2-weighted fluid-attenuated inversion recovery (FLAIR) images for lesion volumetry (appendix e-1). A $10 \times 8 \times 4.5 = 360$ cm^3 ^{1}H-MRSI VOI was then image-guided over the corpus callosum, as shown in figure 1, A and B (appendix e-1). At 2 averages, the ^{1}H-MRSI took 34 minutes and the entire protocol less than an hour.

Segmentation. After segmentation of the MPRAGE images (appendix e-1), the resultant CSF, GM, and WM masks were coregistered with the ^{1}H-MRSI grid using in-house software, as shown in figure 2, A–D, yielding their volume in every voxel in each subject. Their VOI fractions GM_f, WM_f, CSF_f were their respective sums over all 480 voxels divided by the 360 cm^3 VOI volume. Lesion volumes were estimated from the FLAIR images using an automated approach and manual inspection (appendix e-1).

^{1}H-MRSI postprocessing and analyses. Absolute metabolite amounts were obtained using phantom replacement with correction for T1 and T2 relaxation time differences. Global GM and WM concentrations were calculated using linear regression as previously described[5] (appendix e-1). Two-way analysis of variance was used to compare patients to controls in cross-sectional comparisons and random coefficients regression was used to model longitudinal changes (appendix e-1). Linear regression was used to test for correlations between changes in metabolites and in CSF_f, GM_f, WM_f, lesion volume, Expanded Disability Status Scale (EDSS) scores, and relapses (appendix e-1). Statistical significance was defined as a 2-sided p value less than 0.05.

RESULTS Eighteen of the 29 patients met all enrollment criteria. Their demographics at baseline, yearly EDSS scores, and disease-modifying medications are compiled in the table. Their EDSS scores increased by an average of 0.2 (range −2.5 to 2.5), i.e., a rate of 0.05/year. Clinical relapses occurred in 11 patients over the 3 years. Seven patients were scanned at all 7 time points, 9 at 6, and 2 at 5. The 10 controls (mean age 30, range 24–43) were all scanned 4 times each. Mean scanning intervals were 6.4 months in patients and 12.2 months in controls.

Our shim procedure yielded a VOI water line width of 22 ± 4 Hz (mean ± SD). An example of VOI placement and spectra is shown in figure 1. The individual voxels' signal-to-noise ratios, from all 73,440 voxels (153 datasets × 480 spectra each), were NAA = 31 ± 6, Cr = 15 ± 2, Cho = 13 ± 2, and mI = 8 ± 1, with 6.7 ± 1.1 Hz linewidth. Coregistration of the ^{1}H-MRSI matrix to the GM, WM, and CSF masks segmented from the MPRAGE images (figure 2, A–D) revealed that in controls, 1% of voxels comprised >90% GM, 15% had >90% WM, and 86% had minimal, <10%, CSF fraction.

The cross-sectional differences in metabolite levels between patients and controls are shown in figure 3. The average (over all time points) patients' WM Cr, Cho, and mI concentrations, 5.3 ± 0.4, 1.6 ± 0.1, and 5.1 ± 0.7 mM, were higher than the controls' 4.9 ± 0.2, 1.4 ± 0.1, and 4.6 ± 0.4 mM (all $p \leq 0.01$). Patients' values were higher at all time points by a range of 8%–16% for Cr, 4%–13% for Cho, and 7%–17% for mI. The patients' WM NAA was lower with a trend on average (7.4 ± 0.7 mM vs 7.9 ± 0.6 mM, $p = 0.07$), but lower significantly at 4 of the 7 time points (6 months, −8%, $p = 0.05$, 12 months, −7%, $p = 0.02$, 18 months, −9%, $p = 0.05$, and 36 months, −6%, $p = 0.05$). While the average concentrations, over all time points, of GM NAA, Cr, Cho, and mI in patients, 8.8 ± 0.4, 7.1 ± 0.4, 1.3 ± 0.1, and 5.5 ± 0.5 mM, were not different from the controls'

Figure 2 ^{1}H-MRSI–MRI coregistration

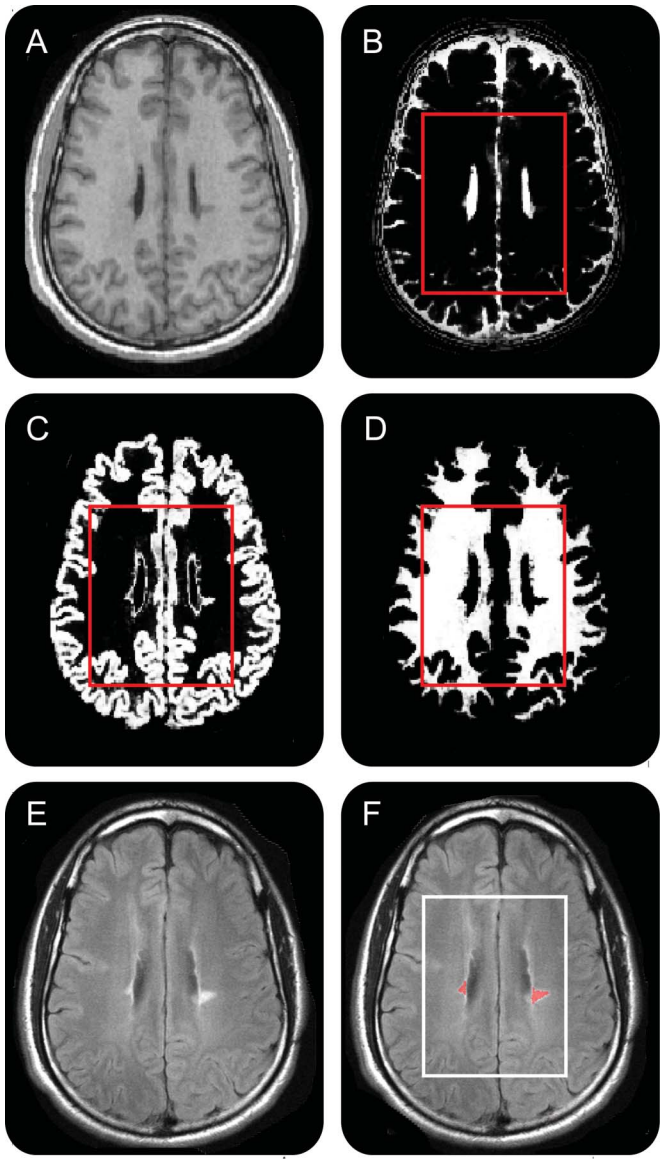

Axial T1-weighted 1-mm-thick magnetization-prepared rapid gradient echo slice (A) from patient 18 and its corresponding CSF (B), gray matter (C), and white matter (D) masks coregistered with the ^{1}H-MRSI volume of interest (VOI) (red frame) and used for obtaining its CSF and tissue fractions. (E) Axial T2-weighted 3.7-mm-thick fluid-attenuated inversion recovery image representing the same plane as (A), overlaid with its lesion mask (red) (F) for VOI (white frame) lesion volumes estimate. ^{1}H-MRSI = proton magnetic resonance spectroscopic imaging.

8.5 ± 0.6, 6.8 ± 0.6, 1.2 ± 0.1, and 5.4 ± 0.6 mM (all $p > 0.16$), there were cross-sectional increases at one time point each of patients' Cho (6 months, +10%, $p = 0.01$), Cr (28 months, +7%, $p = 0.03$), and NAA (28 months, +6%, $p = 0.02$). However, since each of these was observed only once, we are uncertain whether they represent true differences or type I errors.

The serial changes in the distributions of all metabolites are also shown in figure 3. There were significant intracohort rates of change only for patients, who showed increasing WM Cr (0.1 mM/year, $p < 0.001$), Cho (0.02 mM/year, $p = 0.05$), and NAA (0.1 mM/year, $p = 0.04$), as well as decreasing GM Cho (−0.03 mM/year, $p < 0.01$) and mI (−0.1 mM/year, $p = 0.01$). There were no significantly different intercohort (patients' vs controls') rates of change.

Cross-sectional and serial changes in all volumetric metrics are shown in figure 4. Only the patients' average CSF_f, 9.9% ± 1.4%, was different from the controls' 8.4% ± 1.9% ($p = 0.03$). The average GM_f and WM_f were 38.3% ± 1.9% and 51.8% ± 1.9% for patients and 39.6% ± 2.4% and 52.0% ± 3.1% for controls. Patients' average VOI T2 lesion load was 3.9 ± 6.1 cm^3 (median 2.1 cm^3). Intracohort rates of change were significant only in patients, who had increasing CSF_f (0.2%/year) and lesion volume (0.4 cm^3/year) and decreasing WM_f (−0.3%/year) (all $p \leq 0.01$). Although no intercohort rate differences were found, there was a trend for different CSF_f rates ($p = 0.06$).

Finally, the rates of change in GM or WM metabolite levels did not correlate with the rates of change of CSF_f, GM_f, WM_f, lesion volume, EDSS, or relapses, with no trends observed.

DISCUSSION While much is known about MS-associated ^{1}H-MRS changes, their time progression is still unclear due to the limited utility of comparing cross-sectional studies using different patient cohorts and techniques. Despite the reiterated need for serial studies,[1,3,4] practical constraints impede regular follow-up over considerable time periods. To our knowledge, the data here represent the most frequent ^{1}H-MRS follow-up for the longest duration. In addition, most previous studies employed metabolite ratios which decrease the specificity of ^{1}H-MRS, and used single voxels or region-of-interest analysis. In contrast to previous serial ^{1}H-MRS, this study assesses metabolism of a large brain volume, accounts for partial volume effects, and investigates widespread diffuse involvement.

High sensitivity without partial volume bias is achieved by 3D ^{1}H-MRSI in a large (360 cm^3) VOI using each voxel's signal and tissue composition to estimate each metabolite's global concentration per tissue type,[5] thereby boosting the sensitivity, i.e. the precision.[8] It also renders changes in T2-visible lesions insignificant, since they comprise less than 1% of the VOI's volume, as reflected by a lack of correlation between their load and metabolic levels. Therefore, abnormalities detected with this approach must be diffuse throughout the VOI.

Our specific goals were to assign the glial abnormalities previously found in these patients[6] to tissue type and follow this cohort in order to establish the temporal dynamics of their GM and WM metabolism vs controls.

Previously, we showed diffusely elevated Cr, Cho, and mI in the entire VOI of these patients, but could not assign them to a specific tissue type. Given the VOI's ~3:2 WM:GM ratio, however, we conjectured that

Figure 3 Metabolic concentrations in GM and WM

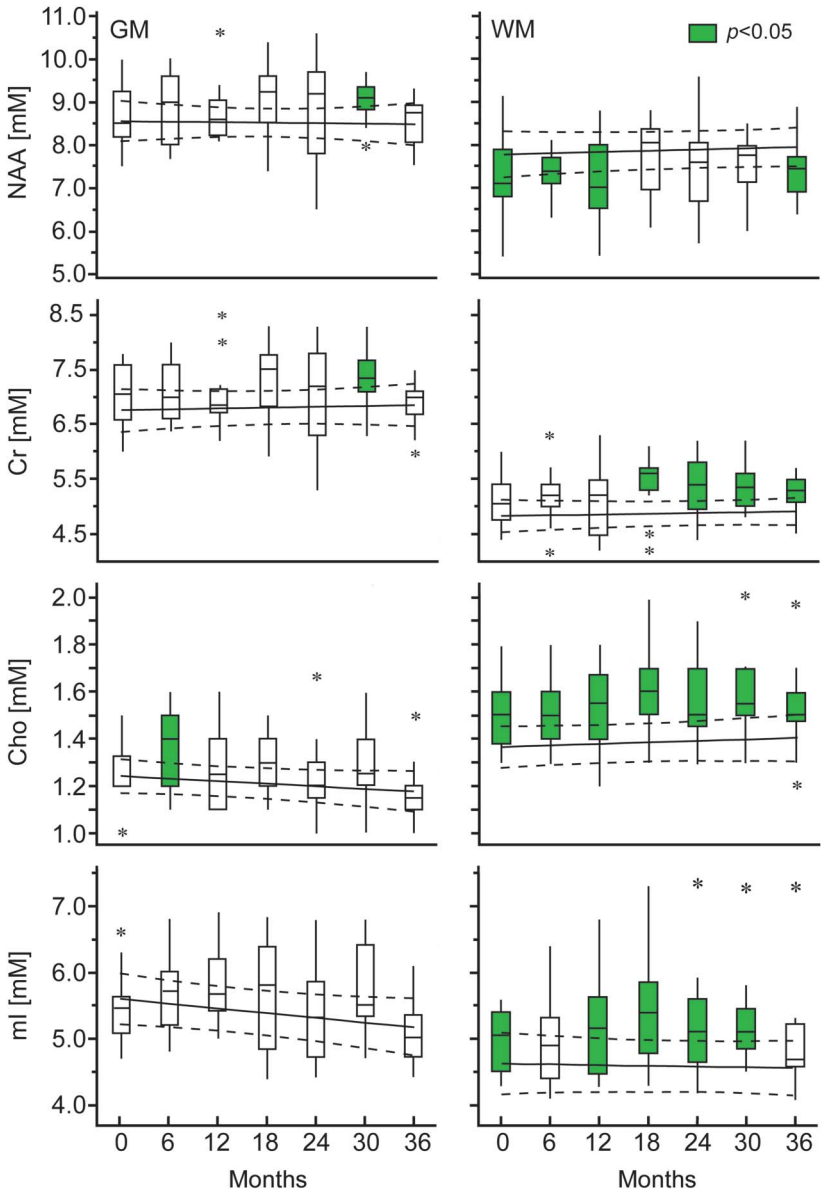

Box plots displaying the 25%, median, and 75% (box), 95% (whiskers), and outliers (*) of the patients' gray matter (GM) and white matter (WM) *N*-acetylaspartate (NAA), creatine (Cr), choline (Cho), and *myo*-inositol (mI) concentrations distributions, overlaid on the regression line of the corresponding average concentrations and 95% confidence intervals (dotted lines) of the controls (to enable visual comparisons since controls were scanned half as many times as the patients). Patients' distributions that are significantly different from the controls' are in green. Significant intracohort rates of change were observed in patients' GM mI and Cho as well as in WM NAA, Cr, and Cho, but there were no intercohort differences in rates.

they represent WM status.[6] This hypothesis is supported by the results here indicating diffuse glial abnormalities in patients' WM relatively early in their RRMS course. The Cr, Cho, and mI concentrations are consistently higher in patients' WM than in controls (on average by 8%, 12%, and 11%, figure 3). Importantly, the increased sensitivity due to separating tissue types helped identify the patients' smaller (6% on average) WM NAA deficits, indicating that axonal impairment accompanies the glial pathology.

Note that the differences in concentrations were on the order of the coefficients of variation, suggesting that they might not always be statistically identifiable due to biological and instrumental "noise." Indeed, higher standard deviations in patients' WM, despite larger sample size, may reflect heterogeneity of disease course or immune or medication responses, suggesting caution in drawing general conclusions from cross-sectional studies, where they can mask subtle pathologic effect. This point may be most pertinent for NAA, which showed the smallest differences, explaining the conflicting reports of both unchanged[9,10] and decreased[11,12] levels in cohorts of similar disease duration. This has important implications for timing and monitoring the neurodegenerative phase of RRMS. In this study, we conclusively show diffuse changes in Cho, Cr, mI, and NAA in the WM of patients with RRMS within ~3 to 6 years from diagnosis.

The single time point GM metabolic differences between patients and controls preclude us from concluding definite GM dysfunction. Previous ^{1}H-MRSI in RRMS has ascribed GM changes to effects of axonal transection associated with WM lesions,[13] or even only to their inflammation.[14] Given the paucity of lesions and relapses in our cohort, it is plausible that GM injury is below the detection threshold since it may still be focal; is still confined to specific structures, e.g., basal ganglia but not the cortex[15]; or is spatially heterogeneous. Such hypotheses, testable in the original 3D data, are beyond the scope here. We conclude, therefore, that at this stage, MS is not characterized by diffuse ^{1}H-MRSI-detectable GM damage.

None of the intercohort rates were significantly different, but patients as a group had significant rates of change. In GM, these were decreases of Cho and mI, and although they may reflect normalizations from a previous elevation, they seem to be driven mainly by a sharp decrease at the last time point, a behavior mimicked by the controls, who have almost identical rates (Cho: −0.03 mM/year for patients and −0.02 mM/year for controls, mI: −0.1 mM/year for both), as seen in figure 3. We are therefore uncertain whether these changes are meaningful or resulted from a systematic bias, also present in controls, where rates were not significant due to their smaller sample size.

In WM, there were significant increases in patients' Cr, Cho, and NAA with much larger intercohort rate differences: fivefold faster Cr and ~ twofold Cho, as well as NAA increases in patients compared to controls. We infer the Cr and Cho as progression of glial pathology and the NAA as concurrent axonal recovery or sparing, possibly due to treatment. This is the first serial report of increasing WM Cr and Cho, and likely reflects progressing glial pathology. In contrast, stable or recovering WM NAA is reported in the majority (10 of 14) of serial studies (e.g., references 16-18), where most patients were

Figure 4 Volumetry

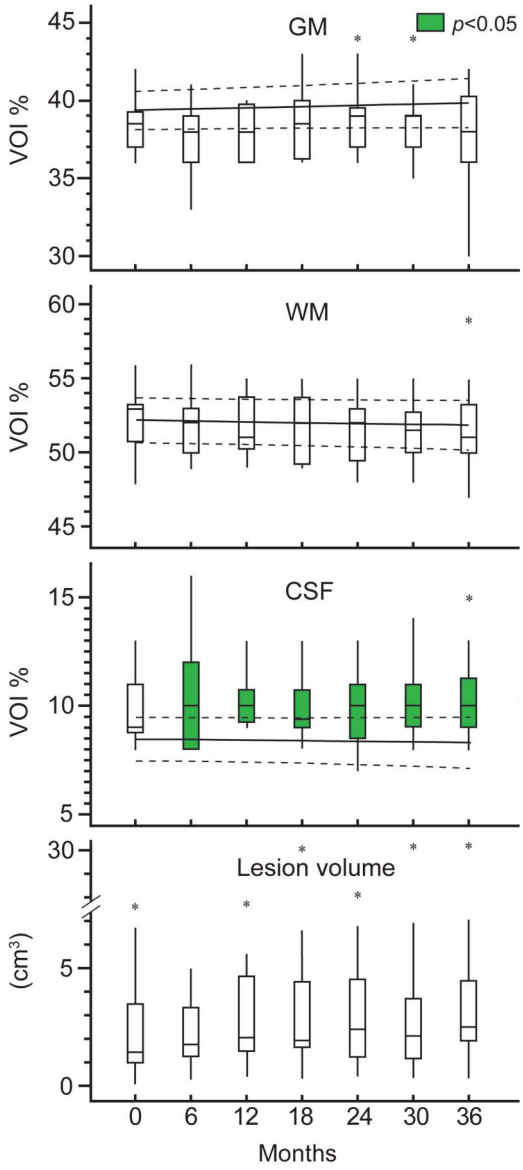

Box plots of patients' volume of interest (VOI) gray matter (GM), white matter (WM), CSF percentage, and lesion volume. Controls are represented with their regression line and 95% confidence intervals (dotted lines). Note that patients' CSF_f was significantly higher than the controls' (green fill). This seems to be driven in part by the patients' lower (but not statistically different) GM_f. Also note that significant decrease in WM_f and increase in CSF_f and lesion volume was observed for patients, as well as a trend for an intercohort difference in the CSF_f rate.

on interferons or glatiramer acetate, the main medications of our cohort and a possible reason for the observed partial NAA recovery. Indeed, WM NAA/Cr increased in interferon-treated[19] and glatiramer acetate–treated[20] patients and declined in nontreated ones. However, as studies with untreated patients are rare, extrapolating these effects to medication per se is speculative. In addition, since most serial studies employed NAA/Cr ratios, Cr elevation, as shown here, may confound concurrent NAA recovery.

The specificity of ^{1}H-MRS can differentiate glial from neuronal injury. In vitro and ex vivo studies have established Cr, Cho, and mI as markers of the former and NAA of the latter.[21,22] The total Cr resonance comprises free creatine and phosphocreatine,[2] found in all cell types, but at higher concentrations in glia than neurons.[21] In MS, high WM phosphocreatine levels have been associated with dysfunctional astrocytes,[23] while recent absolute quantification showed that high Cr levels are due to both free and phosphocreatine and therefore represent gliosis rather than change in energy metabolism.[24] Presence of gliosis in WM has been documented ex vivo[4,25] and corroborated here by the elevated mI, an osmolyte involved in signal transduction in astrocytes[26] and thought to represent astrogliosis.[27] Further glial involvement is suggested by high levels of Cho, which indicate abnormal membrane turnover from demyelination and remyelination.[27] Since Cho is present in all cell walls, however, it may also reflect an ongoing gliosis, as reported in a combined ^{1}H-MRS histopathology study.[28]

In contrast, NAA is almost exclusive to neurons and is therefore considered their marker. NAA levels decline not only with the number of neurons,[28] but also under metabolic stress, so by itself a decrease is nonspecific. In this study, however, we observe concurrent increasing NAA and decreasing WM_f, suggesting that at this stage of RRMS, neuronal dysfunction dominates. Recently, energy failure due to mitochondrial dysfunction has been proposed as a mechanism for neuronal degeneration in MS.[23,29–31] Since NAA is synthesized in the mitochondria, lower levels may reflect reduced mitochondrial activity.[29] If that is driven by inflammation,[31] it is possible that the increasing NAA reflects mitochondrial recovery in response to anti-inflammatory medication. The fact that in the progressive phase of MS neuronal death is independent of inflammation, however, may be related to the steady increase in glial abnormalities, which are more pronounced than NAA loss in early RRMS, and which, unlike NAA, do not seem to abate.

Patients' CSF_f was higher than controls', and increased significantly, reflecting progressive enlargement of lateral and third ventricle and sulci around the medial part of the longitudinal fissure. It was the only rate that showed any evidence of intercohort difference ($p = 0.06$). This type of deep central atrophy characterizes the RRMS phenotype, as it starts early and progresses faster than global atrophy.[32] Patients and controls had statistically indistinguishable WM_f and GM_f, but there was evidence of loss of both tissue types in patients. First, their WM_f had a significant rate of decrease, suggesting accumulating WM atrophy. Second, they had consistently lower GM_f medians and distributions (figure 4), suggesting greater GM contribution to atrophy. Indeed, GM loss may be apparent as early as clinical onset with involvement of the cortex, basal ganglia, and thalamus.[33–35] It is possible that some

WM atrophy is masked by inflammatory changes, such as astrogliosis and remyelination, which are less pronounced in GM,[36,37] as demonstrated by the high WM Cr, Cho, and mI but mostly normal GM metabolite levels.

The postprocessing choice of obtaining global tissue values was to investigate diffuse changes only. Since the original 3D data are available, exploring the contribution of specific structures or regions is feasible. The advantage of our approach, however, was in assessing the largest tissue volumes possible in order to increase the sensitivity, which might otherwise be insufficient to distinguish subtle changes in smaller regions of interest. Second, since our goal was to assess the overall disease load by tissue type, the reported WM changes represent the combined contribution of normal-appearing and "dirty" WM (figure 1D), with unknown contribution of each to the signal. Third, not accounting for lesions in segmentation can result in volume underestimation or overestimation depending on their intensity.[38] Given their low loads in our patients (~4 cm^3), in the most common scenario of misclassification as GM (figure 2C), volume errors would be under 0.7%.[38] Finally, while the reported findings are from a relatively large volume (~40% of the brain's WM and 20% of its GM), they are pertinent only to the regions inside the VOI (figure 1, A and B) and may not be representative of other domains, such as the rest of the cortex.

Glial abnormalities in WM, consistent with myelin breakdown and astrogliosis, are more pronounced than the axonal deficits attributed to dysfunction, such as mitochondrial impairment. In the context of increasing central atrophy and WM tissue loss, the glial changes progressed, while the axons showed partial recovery, presumably in response to treatment. Absolute quantification allowed us to assign metabolic profiles by cell class, which revealed a different time course of glial and neuronal metabolism. This has implications for understanding the natural history of MS as well as monitoring response to treatment paradigms.

AUTHOR CONTRIBUTIONS

Drafting/revising the manuscript for content: Drs. Kirov, Tal, Babb, Herbert, and Gonen. Study concept or design: Drs. Kirov and Gonen. Analysis or interpretation of data: Drs. Kirov and Gonen. Contribution of vital tools: Drs. Tal and Gonen. Acquisition of data: Dr. Kirov. Statistical analysis: Dr. Babb. Study supervision or coordination: Drs. Kirov and Gonen. Obtaining funding: Dr. Gonen.

ACKNOWLEDGMENT

The authors thank the patients and controls who volunteered for this study, and our colleagues Daniel Rigotti and William Wu (assistance with data acquisition), Nikhil Jayawickrama and Emma Gorynski (contribution to segmentation), as well as Nissa N. Perry (patient coordinator).

STUDY FUNDING

This work was supported by NIH grants EB01015, NS29029, and NS050520. Dr. Tal is also supported by the Human Frontiers Science Project.

DISCLOSURE

The authors report no disclosures relevant to the manuscript. Go to Neurology.org for full disclosures.

Received May 9, 2012. Accepted in final form August 6, 2012.

REFERENCES

1. Filippi M, Rocca MA, De Stefano N, et al. Magnetic resonance techniques in multiple sclerosis: the present and the future. Arch Neurol 2011;68:1514–1520.
2. Sajja BR, Wolinsky JS, Narayana PA. Proton magnetic resonance spectroscopy in multiple sclerosis. Neuroimaging Clin N Am 2009;19:45–58.
3. Miller DH, Thompson AJ, Filippi M. Magnetic resonance studies of abnormalities in the normal appearing white matter and grey matter in multiple sclerosis. J Neurol 2003;250:1407–1419.
4. Filippi M, Rocca MA, Barkhof F, et al. Association between pathological and MRI findings in multiple sclerosis. Lancet Neurol 2012;11:349–360.
5. Tal A, Kirov II, Grossman RI, Gonen O. The role of gray and white matter segmentation in quantitative proton MR spectroscopic imaging. NMR Biomed 2012;25:1392–1400.
6. Kirov II, Patil V, Babb JS, Rusinek H, Herbert J, Gonen O. MR spectroscopy indicates diffuse multiple sclerosis activity during remission. J Neurol Neurosurg Psychiatry 2009;80:1330–1336.
7. Poser CM, Paty DW, Scheinberg L, et al. New diagnostic criteria for multiple sclerosis: guidelines for research protocols. Ann Neurol 1983;13:227–231.
8. Kreis R, Slotboom J, Hofmann L, Boesch C. Integrated data acquisition and processing to determine metabolite contents, relaxation times, and macromolecule baseline in single examinations of individual subjects. Magn Reson Med 2005;54:761–768.
9. Vrenken H, Barkhof F, Uitdehaag BM, Castelijns JA, Polman CH, Pouwels PJ. MR spectroscopic evidence for glial increase but not for neuro-axonal damage in MS normal-appearing white matter. Magn Reson Med 2005;53:256–266.
10. Aboul-Enein F, Krssak M, Hoftberger R, Prayer D, Kristoferitsch W. Reduced NAA-levels in the NAWM of patients with MS is a feature of progression: a study with quantitative magnetic resonance spectroscopy at 3 Tesla. PLoS One 2010;5:e11625.
11. He J, Inglese M, Li BS, Babb JS, Grossman RI, Gonen O. Relapsing-remitting multiple sclerosis: metabolic abnormality in nonenhancing lesions and normal-appearing white matter at MR imaging: initial experience. Radiology 2005;234:211–217.
12. Inglese M, Li BS, Rusinek H, Babb JS, Grossman RI, Gonen O. Diffusely elevated cerebral choline and creatine in relapsing-remitting multiple sclerosis. Magn Reson Med 2003;50:190–195.
13. Caramanos Z, DiMaio S, Narayanan S, Lapierre Y, Arnold DL. (1)H-MRSI evidence for cortical gray matter pathology that is independent of cerebral white matter lesion load in patients with secondary progressive multiple sclerosis. J Neurol Sci 2009;282:72–79.
14. Van Au Duong M, Audoin B, Le Fur Y, et al. Relationships between gray matter metabolic abnormalities and white matter inflammation in patients at the very early stage of MS: a MRSI study. J Neurol 2007;254:914–923.
15. Geurts JJ, Reuling IE, Vrenken H, et al. MR spectroscopic evidence for thalamic and hippocampal, but not cortical, damage in multiple sclerosis. Magn Reson Med 2006;55:478–483.
16. Zaaraoui W, Reuter F, Rico A, et al. Occurrence of neuronal dysfunction during the first 5 years of multiple sclerosis is associated with cognitive deterioration. J Neurol 2011;258:811–819.

17. Bellmann-Strobl J, Stiepani H, Wuerfel J, et al. MR spectroscopy (MRS) and magnetisation transfer imaging (MTI), lesion load and clinical scores in early relapsing remitting multiple sclerosis: a combined cross-sectional and longitudinal study. Eur Radiol 2009;19:2066–2074.
18. Tiberio M, Chard DT, Altmann DR, et al. Metabolite changes in early relapsing-remitting multiple sclerosis. A two year follow-up study. J Neurol 2006;253:224–230.
19. Narayanan S, De Stefano N, Francis GS, et al. Axonal metabolic recovery in multiple sclerosis patients treated with interferon beta-1b. J Neurol 2001;248:979–986.
20. Khan O, Shen Y, Bao F, et al. Long-term study of brain 1H-MRS study in multiple sclerosis: effect of glatiramer acetate therapy on axonal metabolic function and feasibility of long-term H-MRS monitoring in multiple sclerosis. J Neuroimaging 2008;18:314–319.
21. Urenjak J, Williams SR, Gadian DG, Noble M. Proton nuclear magnetic resonance spectroscopy unambiguously identifies different neural cell types. J Neurosci 1993;13:981–989.
22. Moffett JR, Namboodiri MA, Neale JH. Enhanced carbodiimide fixation for immunohistochemistry: application to the comparative distributions of N-acetylaspartylglutamate and N-acetylaspartate immunoreactivities in rat brain. J Histochem Cytochem 1993;41:559–570.
23. Cambron M, D'Haeseleer M, Laureys G, Clinckers R, Debruyne J, De Keyser J. White-matter astrocytes, axonal energy metabolism, and axonal degeneration in multiple sclerosis. J Cereb Blood Flow Metab 2012;32:413–424.
24. Hattingen E, Magerkurth J, Pilatus U, Hubers A, Wahl M, Ziemann U. Combined (1)H and (31)P spectroscopy provides new insights into the pathobiochemistry of brain damage in multiple sclerosis. NMR Biomed 2011;24:536–546.
25. Allen IV, McKeown SR. A histological, histochemical and biochemical study of the macroscopically normal white matter in multiple sclerosis. J Neurol Sci 1979;41:81–91.
26. Griffin JL, Bollard M, Nicholson JK, Bhakoo K. Spectral profiles of cultured neuronal and glial cells derived from HRMAS (1)H NMR spectroscopy. NMR Biomed 2002;15:375–384.
27. Bakshi R, Thompson AJ, Rocca MA, et al. MRI in multiple sclerosis: current status and future prospects. Lancet Neurol 2008;7:615–625.
28. Bitsch A, Bruhn H, Vougioukas V, et al. Inflammatory CNS demyelination: histopathologic correlation with in vivo quantitative proton MR spectroscopy. AJNR Am J Neuroradiol 1999;20:1619–1627.
29. Paling D, Golay X, Wheeler-Kingshott C, Kapoor R, Miller D. Energy failure in multiple sclerosis and its investigation using MR techniques. J Neurol 2011;258:2113–2127.
30. Lassmann H, van Horssen J. The molecular basis of neurodegeneration in multiple sclerosis. FEBS Lett 2011;585:3715–3723.
31. Nikic I, Merkler D, Sorbara C, et al. A reversible form of axon damage in experimental autoimmune encephalomyelitis and multiple sclerosis. Nat Med 2011;17:495–499.
32. Simon JH. Brain atrophy in multiple sclerosis: what we know and would like to know. Mult Scler 2006;12:679–687.
33. Dalton CM, Chard DT, Davies GR, et al. Early development of multiple sclerosis is associated with progressive grey matter atrophy in patients presenting with clinically isolated syndromes. Brain 2004;127:1101–1107.
34. Calabrese M, Atzori M, Bernardi V, et al. Cortical atrophy is relevant in multiple sclerosis at clinical onset. J Neurol 2007;254:1212–1220.
35. Audoin B, Davies GR, Finisku L, Chard DT, Thompson AJ, Miller DH. Localization of grey matter atrophy in early RRMS: a longitudinal study. J Neurol 2006;253:1495–1501.
36. Valsasina P, Benedetti B, Rovaris M, Sormani MP, Comi G, Filippi M. Evidence for progressive gray matter loss in patients with relapsing-remitting MS. Neurology 2005;65:1126–1128.
37. Ceccarelli A, Rocca MA, Pagani E, et al. A voxel-based morphometry study of grey matter loss in MS patients with different clinical phenotypes. Neuroimage 2008;42:315–322.
38. Chard DT, Jackson JS, Miller DH, Wheeler-Kingshott CA. Reducing the impact of white matter lesions on automated measures of brain gray and white matter volumes. J Magn Reson Imaging 2010;32:223–228.